Supporting Information

Temperature-Responsive Peptide-Nucleotide Coacervates

Tiemei Lu[1], Karina K. Nakashima[1], Evan Spruijt[1]*

[1]Radboud University, Institute for Molecules and Materials, Heyendaalseweg 135, 6525 AJ Nijmegen, the Netherlands. *Correspondence: e.spruijt@science.ru.nl

Supplementary Table

Table S1. Molecular structures of polycations and polyanions used in this study.

Negatively charged components	Structure	Positively charged components	Structure
ATP	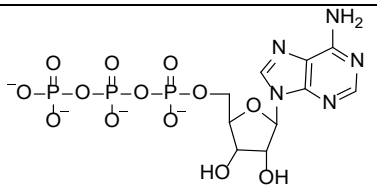	PLys	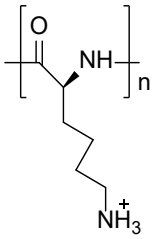
GTP	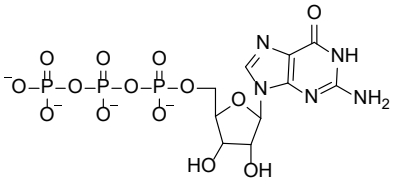		
CTP	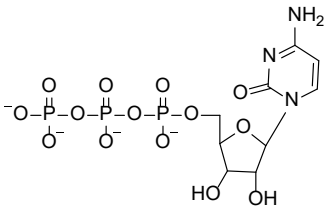	PArg	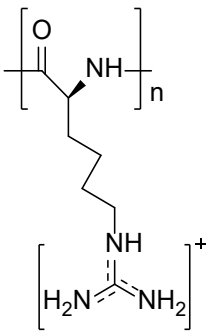
dTTP	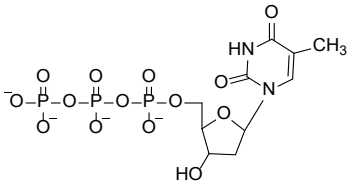		
UTP	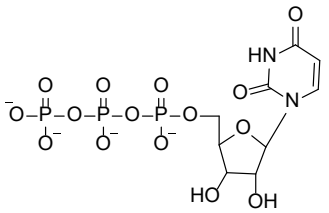		
TPP	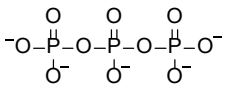		

Supplementary Figures

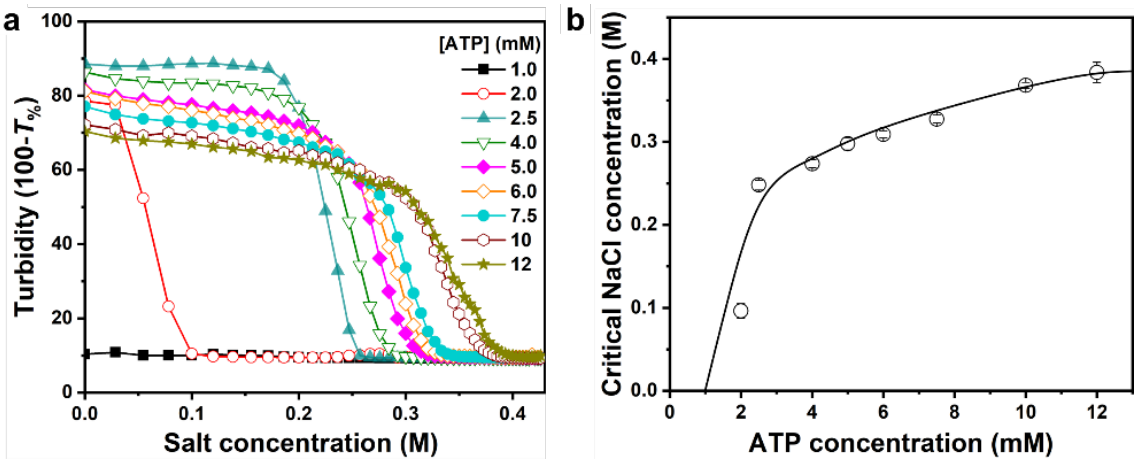

Figure S1. (a) Turbidity of ATP/PLys mixtures as a function of the NaCl concentration (turbidity-based titrations from low to high salt concentration, measured at 22 ℃). (b) Critical salt concentration for ATP coacervates with 5 mM PLys, determined from turbidity-based titrations in (a).

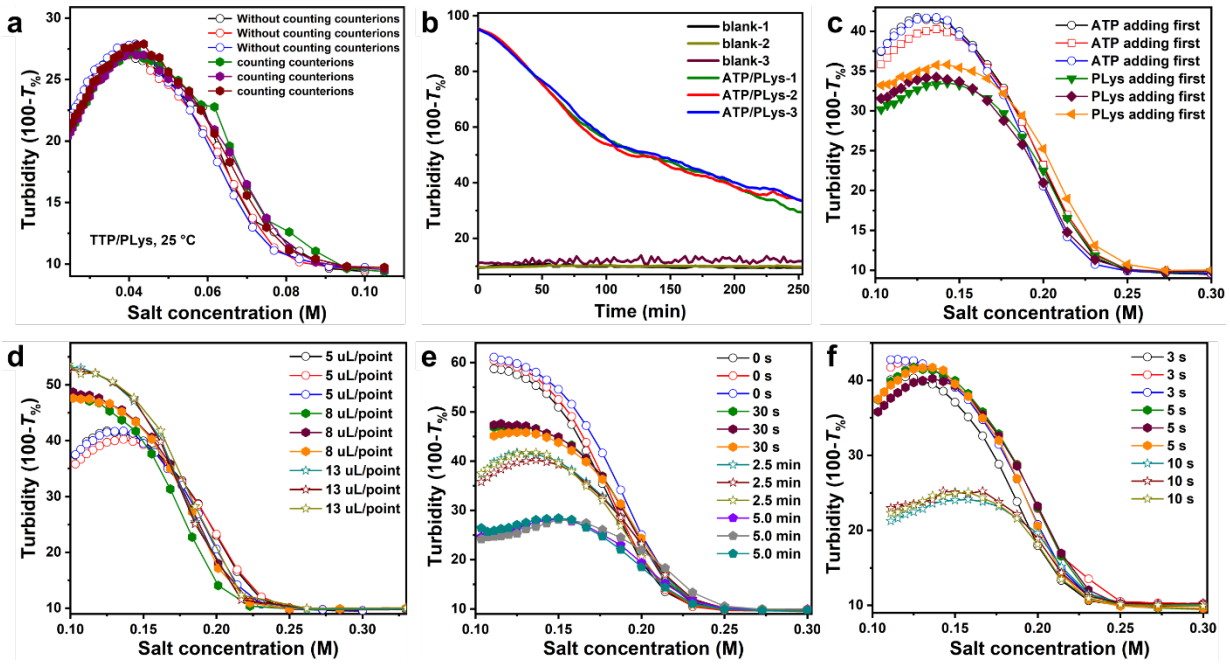

Figure S2. (a) Turbidity of TTP/PLys mixtures at 25 ℃ as a function of salt concentration without and with counting counterions. (b) Turbidity of ATP-PLys coacervate droplets and blank sample (without ATP and PLys) at salt concentration of 0 M as a function of time. (c-f) The effects of different titration conditions on turbidity of ATP/PLys mixtures as a function of salt concentration curves at 25 ℃: (c) different adding order of ATP and PLys; (d) different titration rates (the lowest value of the plate reader is 5 μL/point); (e) different settling time; (f) different shaking duration.

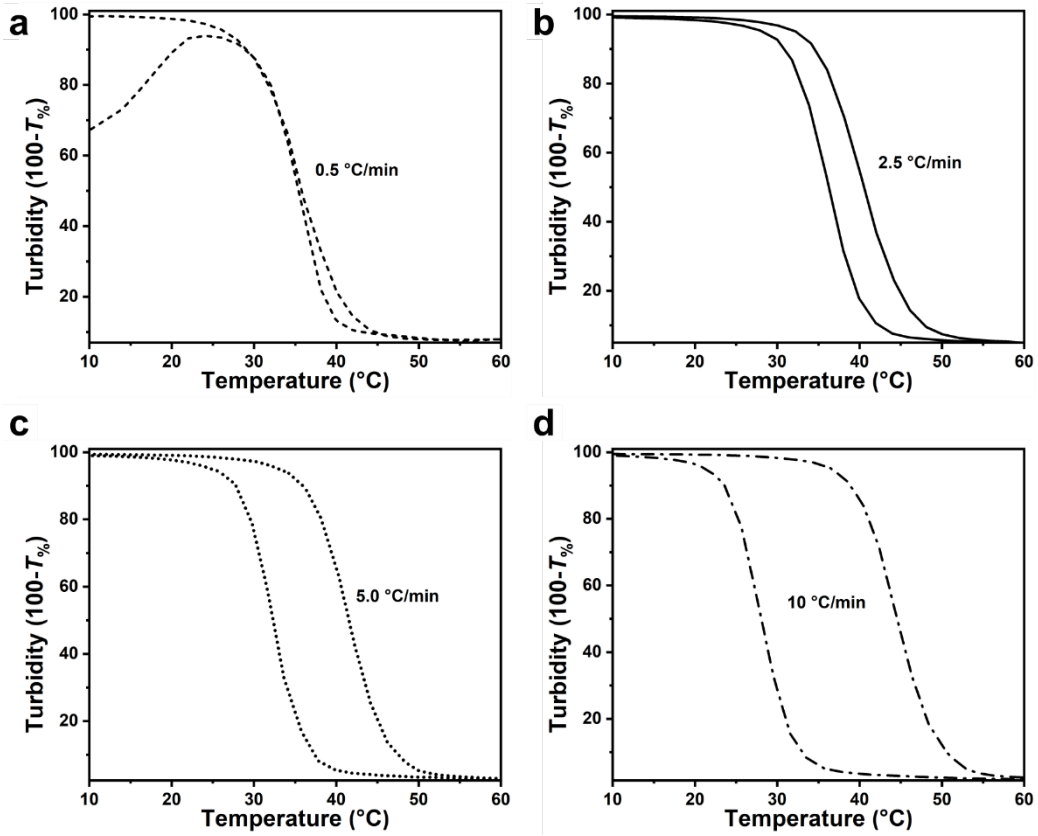

Figure S3. Plots showing temperature-dependent decrease and increase of the turbidity from 10 ℃ to 60 ℃ and back to 10 ℃ of ATP/PLys at salt concentration of 0.22 M with different temperature increasing rates: (a) 0.5 ℃/min; (b) 2.5 ℃/min; (c) 5.0 ℃/min; (d) 10 ℃/min.

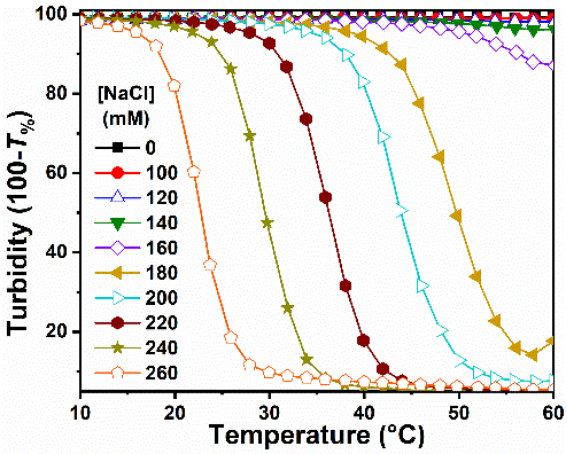

Figure S4. Plots showing temperature-dependent increase of the turbidity from 60 to 10 ℃ of ATP/PLys coacervates at different salt concentration.

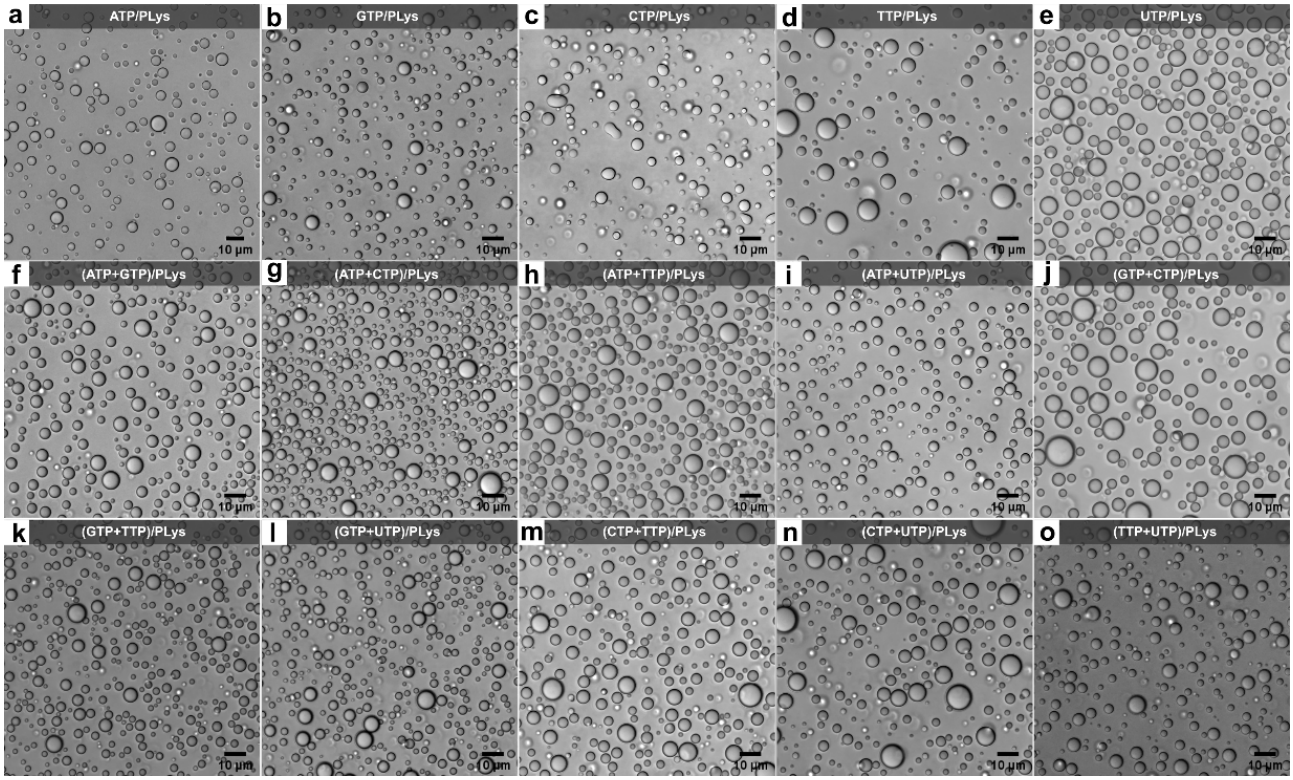

Figure S5. Microscope images of coacervate droplets formed by NTPs with PLys.

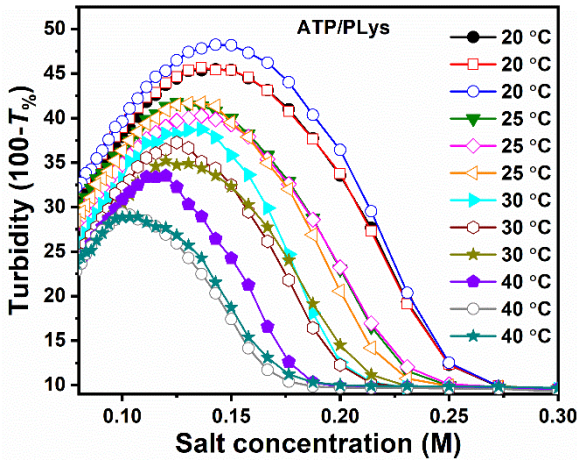

Figure S6. An example of turbidity of NTPs with PLys as a function of salt concentration from 20 to 40 ℃: ATP/PLys (turbidity-based titrations from high to low salt concentration).

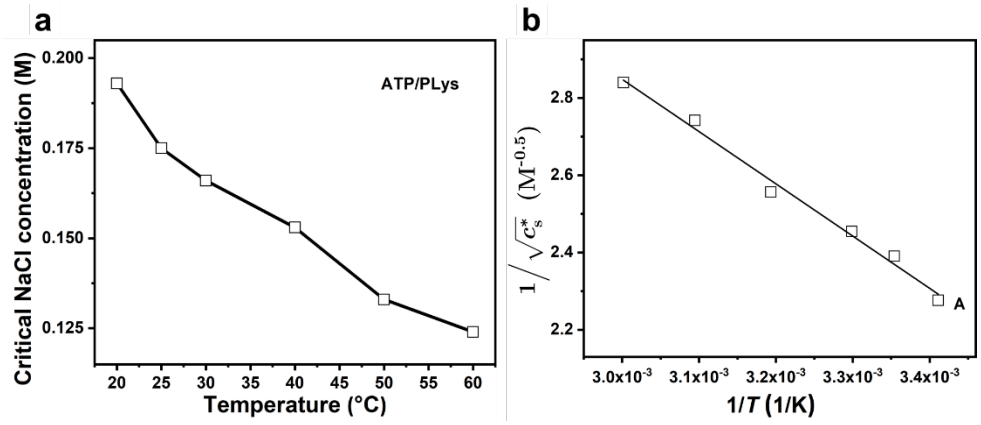

Figure S7. (a) Temperature-dependence of c_s^* of ATP with PLys by UV-Vis spectra. (b) Linearization of (a) according to eq 4.

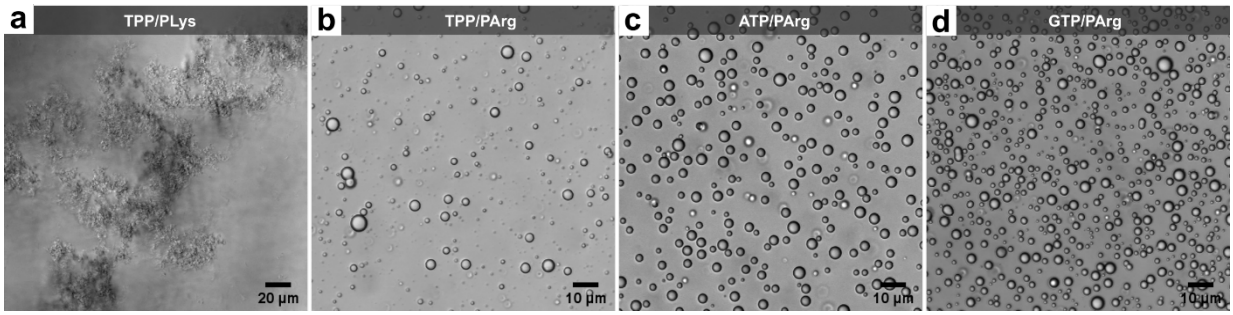

Figure S8. Microscope images of coacervate droplets formed by TPP, ATP and GTP with PLys and PArg, respectively.

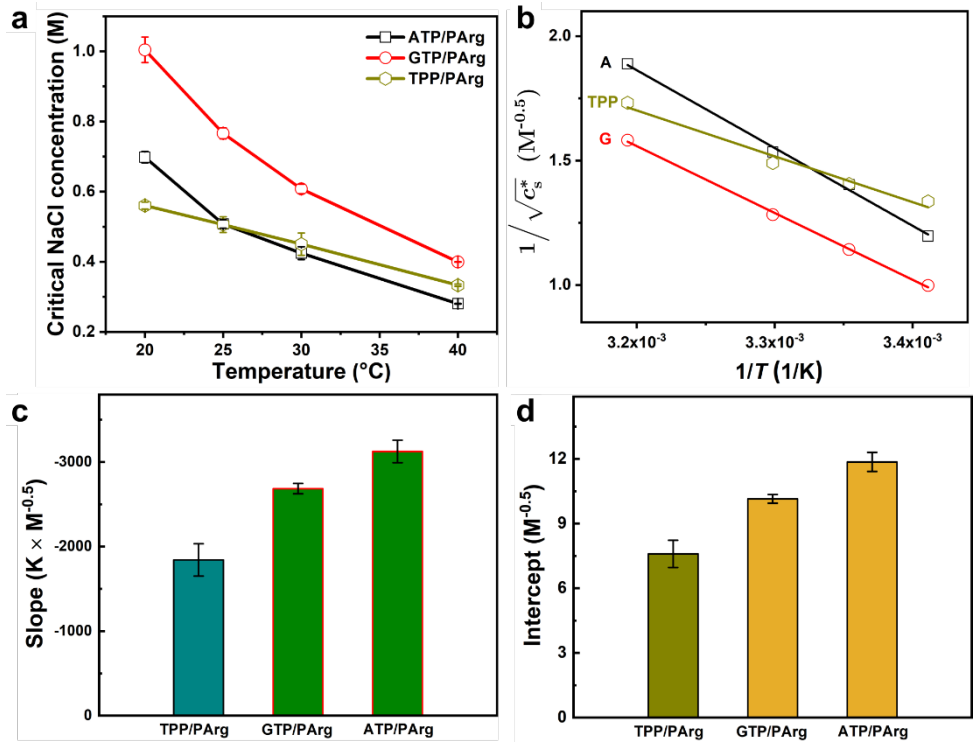

Figure S9. UCST behavior of coacervates of ATP, GTP and TPP with PArg. (a) Temperature-dependence of c_s^* of ATP, GTP and TPP with PArg coacervates. (b) Linearization of (a) according to eq 4. (c) Slopes and (d) intercepts of linear fits of the data in (b).

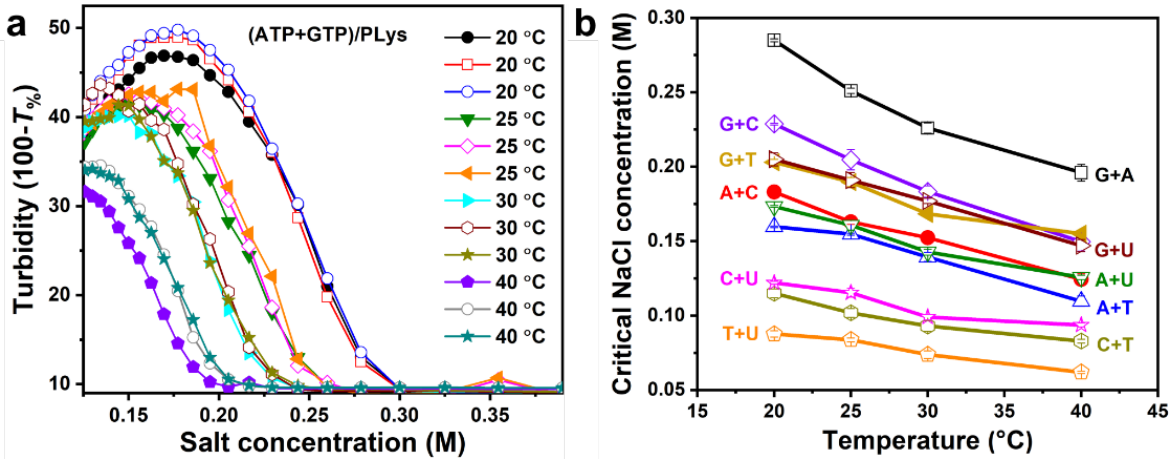

Figure S10. (a) An example of turbidity of hybrid NTPs with PLys as a function of salt concentration: (ATP+GTP)/PLys (turbidity-based titrations from high to low salt concentration). (b) Temperature-dependence of c_s^* of hybrid NTPs with PLys, determined from turbidity-based titrations.

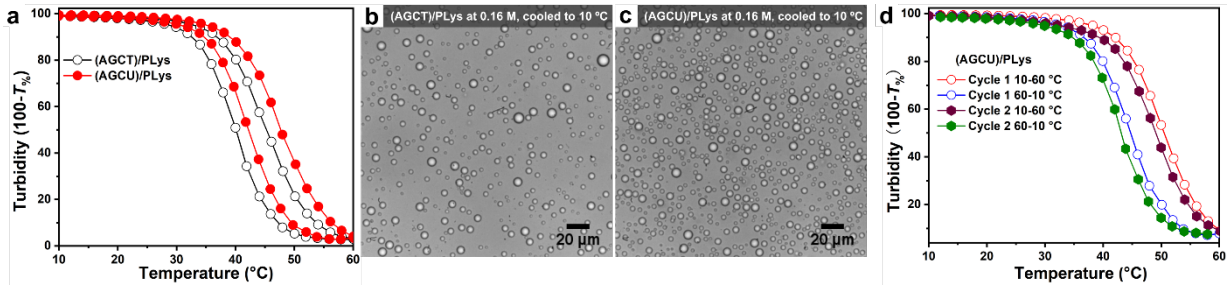

Figure S11. (a) Plots showing temperature-dependent decrease and increase of the turbidity from 10 °C to 60 °C and back to 10 °C of (AGCT)/PLys and (AGCU)/PLys coacervates at salt concentration of 0.16 M. (b, c) Microscope images of (AGCT)/PLys and (AGCU)/PLys coacervate droplets after completing a full cycle of heating and cooling, when the temperature reached 10 °C again. (d) Two cycles of the turbidity from 10 °C to 60 °C and back to 10 °C of (AGCU)/PLys coacervates at salt concentration of 0.16 M.

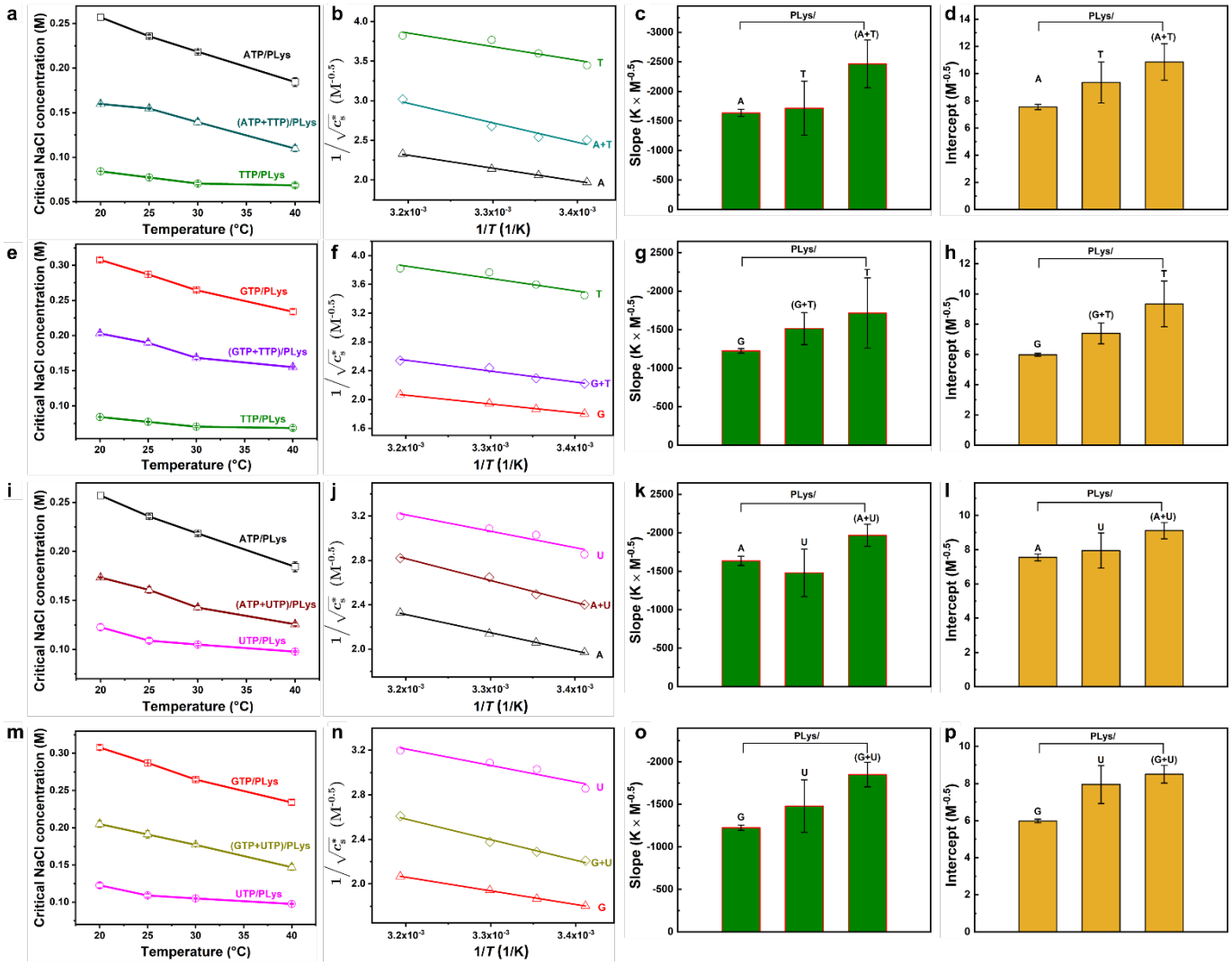

Figure S12. UCST behavior of hybrid NTPs-PLys coacervates. (a, e, i, m) Temperature-dependence of c_s^* of ATP, TTP and their mixture with PLys; GTP, TTP and their mixture with PLys; ATP, UTP and their mixture with PLys; GTP, UTP and their mixture with PLys, respectively. (b, f, j, n) Linearization of (a, e, i, m) according to eq 4. (c, g, k, o) Slopes and (d, h, l, p) intercepts of linear fits of the data in b, f, j and n, respectively.

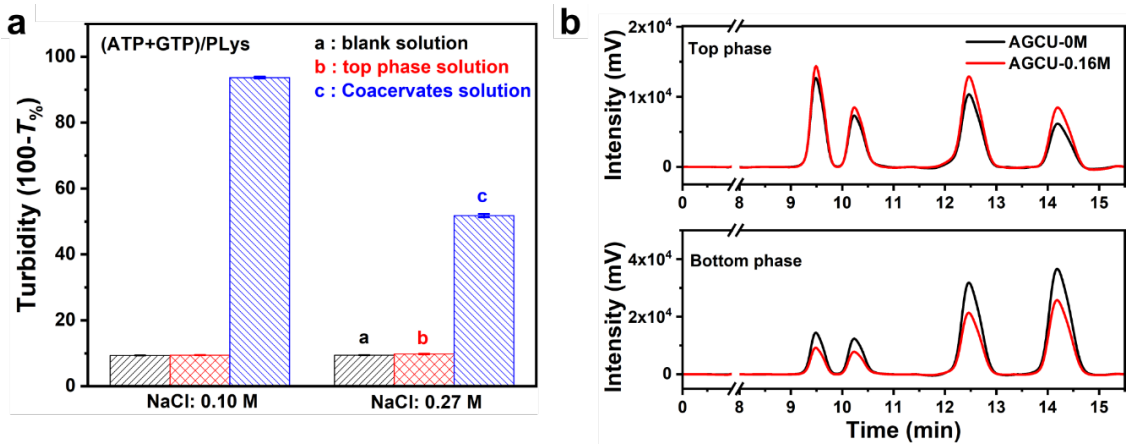

Figure S13. (a) Turbidity of blank solution (without ATP, GTP and PLys), top phase solution from (ATP+GTP)/PLys coacervate droplets after low-speed centrifugation and (ATP+GTP)/PLys coacervate droplets solution at salt concentration of 0.10 M and 0.27 M, respectively. (b) HPLC analysis of the top phase and bottom phase of (AGCU)/PLys coacervate droplets with two different salt concentration after centrifugation.

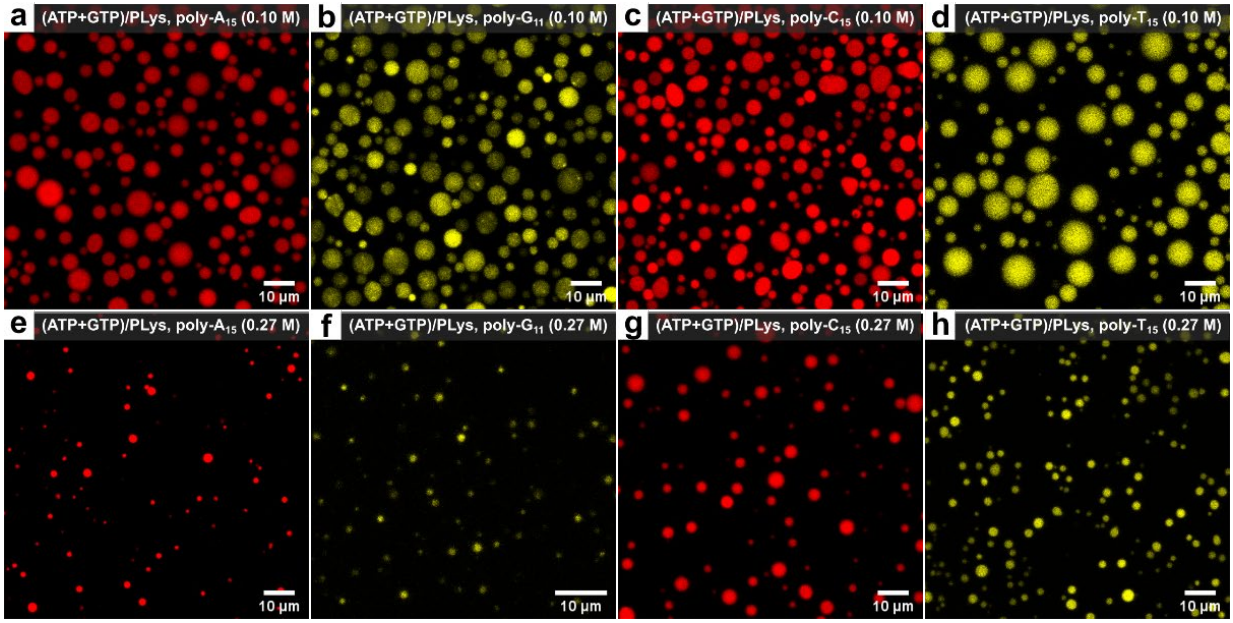

Figure S14. Partitioning of four different labelled DNA oligonucleotides guest molecules in (ATP+GTP)/PLys coacervate droplets with two different salt concentration visualized by confocal fluorescence microscopy: (a) poly-A_{15}, 0.10 M; (b) poly-G_{11}, 0.10 M; (c) poly-C_{15}, 0.10 M; (d) poly-T_{15}, 0.10 M; (e) poly-A_{15}, 0.27 M; (f) poly-G_{11}, 0.27 M; (g) poly-C_{15}, 0.27 M; (h) poly-T_{15}, 0.27 M.

Supplementary Movies

Movie S1. The dissolution process of ATP/PLys coacervate droplets at salt concentration of 0.22 M by increasing the temperature from 20 to 60 ℃. Images were recorded with a default frequency of 1 second/picture, heating rate of 2.5 ℃/min. In this movie, the replay speed is 40 times faster than the recorded experiment (a time stamp is shown at the top right).

Movie S2. The formation process of ATP/PLys coacervate droplets at salt concentration of 0.22 M by decreasing the temperature from 60 to 20 ℃. Images were recorded with a default frequency of 1 second/picture, cooling rate of 2.5 ℃/min. In this movie, the replay speed is 40 times faster than the recorded experiment (a time stamp is shown at the top right).